

1 **A matrix matched reference material for validating petroleum Re-Os**

2 **measurements**

3
4 Junjie Liu (junjie.liu@durham.ac.uk), David Selby (david.selby@durham.ac.uk, +44 (0) 191
5 33 42294)

6 Department of Earth Sciences, Durham University, Durham, DH1 3LE, UK

7 8 **Abstract**

9
10 This study presents two matrix-matched reference materials developed for petroleum Re-Os
11 measurements. We present the Re and Os mass fractions and $^{187}\text{Re}/^{188}\text{Os}$ and $^{187}\text{Os}/^{188}\text{Os}$
12 values (ratio of the number of atoms of the isotopes) for repeatedly measured aliquots (ca.
13 120 - 150 mg test portions) of the NIST Research Material 8505 (RM 8505) crude oil, and its
14 asphaltene and maltene fractions, and ~ 90 g of homogeneous asphaltene powder isolated
15 from this oil. Measurements were performed using the Carius Tube - Isotope Dilution -
16 Negative Thermal Ionization Mass Spectrometry methodology. The RM 8505 crude oil
17 contains $1.98 \pm 0.07 \text{ ng g}^{-1}$ Re and $25.0 \pm 1.1 \text{ pg g}^{-1}$ Os, with Re-Os isotope amount ratios of
18 452 ± 6 for $^{187}\text{Re}/^{188}\text{Os}$ and 1.51 ± 0.01 for $^{187}\text{Os}/^{188}\text{Os}$ ($n = 20$, 95% conf.). The
19 homogeneous asphaltene sample contains $16.52 \pm 0.10 \text{ ng g}^{-1}$ Re and $166.0 \pm 0.9 \text{ pg g}^{-1}$ total
20 Os, and possesses isotope amount ratios of 574 ± 3 for $^{187}\text{Re}/^{188}\text{Os}$ and 1.64 ± 0.01 for
21 $^{187}\text{Os}/^{188}\text{Os}$ ($n = 24$, 95% conf.). The intermediate precision of these data makes the RM 8505
22 whole oil and the (~ 90 g) homogenised asphaltene appropriate petroleum matrix-matched
23 reference materials for Re-Os measurements. The asphaltene fraction of the oil is the main
24 carrier of Re and Os of the RM 8505 whole oil and caution is suggested in using asphaltene
25 and maltene fractions of a single oil for Re-Os geochronology.

26
27
28
29
30
31
32
33
34
35
36
37
38
39
40
41
42
43
44
45
46
47
48
49
50

Key words: petroleum Re-Os measurements; reference material; N-TIMS; RM 8505 crude oil; homogenised asphaltene powder

1 Introduction

Since its inaugural application to the Polaris Mississippi Valley Type Pb-Zn deposit (Selby *et al.* 2005) and the Giant Oil Sands of Alberta, Canada (Selby and Creaser 2005), the rhenium-osmium (Re-Os) radioisotope system has been applied to many petroleum systems worldwide (Selby *et al.* 2007; Finlay *et al.* 2010; Finlay *et al.* 2011; Cumming *et al.* 2012; Finlay *et al.* 2012; Rooney *et al.* 2012; Lillis and Selby 2013; Cumming *et al.* 2014; Ge *et al.* 2016; Georgiev *et al.* 2016). These studies have demonstrated that the Re-Os isotope systematics of petroleum (crude oil, bitumen) allow the direct dating of the processes related to petroleum generation and evolution, and also provide insights into the source of the petroleum. Laboratory studies have also been carried out on the Re-Os isotope systematics of crude oil fractions (Selby *et al.* 2007; Mahdaoui *et al.* 2013; Mahdaoui *et al.* 2015; Georgiev *et al.* 2016). These studies have discussed the possible influences of geological processes on the Re-Os systematics of petroleum and its application to petroleum systems, e.g. the timing of oil generation, the precipitation of asphaltene, and the effect of contact with basinal fluids. Previous Re-Os petroleum studies have utilized a wide range of sample types. They include not only conventional crude oil, but also the altered forms, e.g. bitumen of different origins. The Re-Os measurement methods were initially setup for rock samples, e.g. sulphides and organic-rich mudrocks (Cohen *et al.* 1999; Reisberg and Meisel 2002; Marques 2013; Zimmerman *et al.* 2014) and then adapted for the specific characteristics of petroleum

51 samples (Selby *et al.* 2005; Mahdaoui *et al.* 2013; Sen and Peucker-Ehrenbrink 2014;
52 Georgiev *et al.* 2016). In general, current petroleum Re-Os measurement procedures adopt
53 similar chemical purification procedures among different laboratories with the main
54 differences being the digestion (i.e. choice of vessels and acids) and mass spectrometry (N-
55 TIMS and ICP-MS) methods. The two noteworthy characteristics of petroleum samples that
56 the protocols have to deal with are the low mass fractions (abundances) of Re ($\leq 1 \text{ ng g}^{-1}$) and
57 Os ($\sim 10 \text{ pg g}^{-1}$) of many oils (see Selby *et al.* 2007) and the high pressure during the
58 digestion.

59

60 Petroleum samples are usually digested in closed-system (Carius tubes and Anton Paar High
61 Pressure Asher (HPA-S) vessels) with strong oxidizing acids. The digestion process should
62 ensure the complete destruction of the organic matrix and the achievement of the highest
63 oxidation state of all Os, i.e. OsO_4 , to permit the equilibrium of the sample and spike Os. The
64 most commonly used digestion reagent is concentrated nitric and hydrochloric acid in the
65 form of inverse *aqua regia*. The addition of hydrogen peroxide is demonstrated to increase
66 the efficiency of sample digestion and the mass spectrometer Os signal (Li *et al.* 2011).
67 However, it also increases the risk of Carius tube rupture during digestion. The low Re and
68 Os concentrations of many crude oils require a large amount of sample and low procedural
69 blanks to obtain accurate and precise data. However, the high pressure generated by the
70 formation of carbon dioxide during the digestion process limits the amount of sample that can
71 be handled with the current digestion technique. The HPA-S method has been used to digest
72 up to 0.45 g of crude oil effectively (Georgiev *et al.* 2016) and 1 g pumpkin seed oil (90 ml
73 quartz vessel, Bandoniene *et al.* 2013) and it can also digest samples in short times (overnight
74 or $\sim 2\text{-}3$ hrs). Further, a recent study described the design of re-useable Carius tubes (Qi *et al.*
75 2013). Both Carius tubes and HPA-S methods can yield low blanks, with the blanks primarily

76 controlled by the reagents used. Importantly, reuse of digestion vessels increase the
77 probability of variable blanks, which can hamper the application of most appropriate blank
78 correction. When tubes are not reused, the Carius tube - inverse aqua regia methodology
79 typically yields low Re and Os blanks across different labs, e.g. generally lower than 10 pg
80 for Re and 50 - 200 fg for Os (e.g. Cumming *et al.* 2014 and this study, Table 1), less than 3
81 pg Re and 2 pg Os (Steven *et al.* 2015), and 3.7 ± 4.7 pg Re and 340 ± 226 fg Os (Georgiev
82 *et al.* 2016).

83

84 After sample digestion and spike-sample equilibration, the Os fractions are typically
85 extracted with an organic solvent and purified by micro-distillation (Cohen and Waters 1996;
86 Birck *et al.* 1997), with the Re fractions being purified by anion exchange chromatography
87 (Morgan *et al.* 1991; Selby and Creaser 2001). The Re and Os isotope compositions of the
88 purified Re and Os fractions from samples are determined by Negative Thermal Ionization
89 Mass Spectrometry (N-TIMS) and/or (Multi-Collector) Inductively Coupled Plasma Mass
90 Spectrometry (MC-ICP-MS/ICP-MS) (Creaser *et al.* 1991; Völkening *et al.* 1991; Reisberg
91 and Meisel 2002; Meisel *et al.* 2003; Walczyk 2004; Nowell *et al.* 2008). The MC-ICP-
92 MS/ICP-MS permits faster isotope ratio determination and simpler elemental purification
93 chemistry. However, the N-TIMS methodology is a more appropriate reference technique for
94 Os isotope ratio measurement because of its advantage of high ionisation efficiency, no
95 significant memory and small mass fractionation which are especially important for oils that
96 often possess low mass fractions of Os.

97

98 The pursuit of simple, rapid and low uncertainty Re-Os measurement of petroleum and the
99 demand for both intra-laboratory calibration and inter-laboratory comparison are driven by
100 the increasing interest and application of petroleum Re-Os measurement. Considering the

101 unique nature of petroleum samples, e.g. easy to digest, significant CO₂ generated during
102 digestion and typically low Re and Os mass fractions, a matrix-matched reference material is
103 needed for petroleum Re-Os measurement method development and validation. Some
104 progress has already been made (Sen and Peucker-Ehrenbrink 2014). In this study, we
105 present Re-Os data for the National Institute of Standards and Technology (NIST) vanadium
106 Research Material 8505 crude oil and a homogeneous asphaltene sample (~ 90 g) isolated
107 from the RM 8505 oil, to demonstrate their use as appropriate petroleum matrix-matched
108 reference materials for Re-Os measurement. These two samples are repeatedly analysed for
109 their Re and Os mass fractions and isotope ratios via the Carius Tube - Isotope Dilution -
110 NTIMS methodology. In addition, based on the Re-Os analysis of individually separated
111 asphaltene and maltene fractions in this study, we further confirm that asphaltene is the main
112 carrier of Re and Os within crude oils, and that there is negligible Re and Os in the volatile
113 fraction (at 80 °C) of this oil.

114

115 **2 Samples preparation**

116

117 Research Material 8505 is a Venezuelan crude oil with currently (year of 2017)
118 approximately 100 bottles of 250 ml in stock which should last for more than ten years given
119 current sales rate. This longevity estimate may reduce if the Research Material 8505 is
120 adopted for more for research methods other than vanadium, as proposed here for Re-Os
121 research. The oil was produced in 1983 and received from the Scallop Petroleum Company, a
122 subsidiary of Royal Dutch Shell. No geological details concerning the origin of this oil are
123 available. The predominant source rocks (95% source of Venezuelan's crude oil) of
124 Venezuela are the Upper Cretaceous (Cenomanian-Turonian-Coniacian, 100 – 86 Ma) La
125 Luna Formation and its age equivalents, with only minor contributions from Palaeocene,

126 Eocene and Miocene source rocks (James 1990 2000; Summa *et al.* 2003). Oil generation
127 from the La Luna Formation is considered to have occurred from the Early Eocene onwards
128 (≤ 56 Ma), with the majority of the oil having been generated since the Miocene (James 2000;
129 Summa *et al.* 2003).

130

131 In this study, four sample types were repeatedly analysed for their Re and Os mass fractions
132 and isotope (amount) ratios, i.e. the RM 8505 crude whole oil, the individually separated
133 asphaltene and maltene fractions from RM 8505, and a homogenised asphaltene sample. Five
134 bottles of RM 8505 crude oil were used and subtitled A, B, C, D and E.

135

136 The asphaltene fraction of an oil is defined as the insoluble fraction of oil in *n*-alkanes and
137 the maltene is the soluble fraction. The separation in this study is done by adding 40 ml of *n*-
138 heptane to ~ 1 g of whole oil (Speight 2004; Selby *et al.* 2007). The *n*-heptane and crude oil
139 were thoroughly mixed and left on a rocker overnight at room temperature. The next day the
140 mixture was centrifuged at 3500 rpm for 15 minutes. The precipitated asphaltene was
141 separated by decanting the maltene-bearing *n*-heptane. The asphaltene fraction was
142 transferred to a glass vial using chloroform and dried at 60 °C. The maltene fractions were
143 recovered by evaporating the *n*-heptane at 80 °C in a glass vial.

144

145 To produce the homogenised asphaltene powder, the asphaltene fraction of ~ 1 kg of RM
146 8505 oil from all five bottles was isolated and homogenised. The isolation procedure of the
147 asphaltene was generally the same as the *n*-heptane method described above. The difference
148 is that the *n*-heptane asphaltene-maltene mixture was filtered through 0.45 μm Whatman
149 glass microfibre filter instead of being centrifuged. The dried asphaltene was ground to fine
150 powder ($< 212 \mu\text{m}$) using an agate pestle and mortar, homogenised, and then evenly

151 distributed into 12 glass bottles with 7.5 g of asphaltene placed into each bottle. This amount
152 asphaltene will permit 50 analyses if using 150 mg aliquots per Re-Os analysis. All of the 12
153 glass vials are retained at Durham University and can be obtained via David Selby, which is
154 expected to last for five to ten years. The asphaltene accounts for ~ 11% of the whole oil. For
155 the bulk separated asphaltene, the maltene was not recovered from *n*-heptane or measured for
156 Re-Os.

157

158 For bottle A, six Re-Os analyses on each of the whole oil, individually separated asphaltene
159 and maltene fractions were conducted. For bottles B, C, D, and E, three Re-Os analyses were
160 carried out for each of the three sample types from every bottle. The asphaltene and maltene
161 samples represent paired petroleum fractions from the separation of ~ 1 g crude oil by *n*-
162 heptane. They are not separated from the whole oil Re-Os analysis samples from the same
163 bottle. In total we present the data of eighteen Re-Os analyses of each sample type for the
164 five bottles. In addition, Re-Os analyses were performed on two samples taken from each of
165 the twelve bottles of the homogenised asphaltene powder.

166

167 **3 Measurement procedure**

168

169 The Re and Os mass fractions and Re-Os isotopic systematics were determined by the Isotope
170 Dilution – Negative Thermal Ionisation Mass Spectrometry (ID-NTIMS) method at Durham
171 University in the Laboratory for Source Rock and Sulphide Geochronology and
172 Geochemistry (a member of the Durham Geochemistry Centre). The analytical protocols are
173 based on those developed in previous studies (Creaser *et al.* 1991; Shirey and Walker 1995;
174 Birck *et al.* 1997; Selby and Creaser 2001; Selby *et al.* 2007).

175

176 The sample test portion sizes used for each Re-Os analysis were ~ 150 mg of whole oil and
177 maltene, ~ 120 mg of the individually separated asphaltene and ~ 150 mg for the
178 homogenised asphaltene powder. The solid asphaltenes were weighed using weighing paper.
179 The viscous crude oil and maltene were weighed in small glass vials (~ 3 ml and 4.5 g) and
180 then transferred into a pre-cleaned (with step 1 by 5% H₂O₂, step 2 by 8 mol l⁻¹ HNO₃, step 3
181 by high purity water) Carius tubes with the aid of ~ 1 ml chloroform, which was evaporated
182 at 60°C.

183
184 After adding a known amount of ¹⁸⁵Re + ¹⁹⁰Os mixed tracer solution, the samples were
185 dissolved and equilibrated in Carius tubes using inverse *aqua regia* (3 ml 12 mol l⁻¹ HCl + 6
186 ml 16 mol l⁻¹ HNO₃) at 220 °C for 24 hrs. A solvent extraction methodology was used to
187 isolate the Os from the digested solution using 3 x 3 ml aliquots of chloroform. The Os was
188 then back-extracted from chloroform with 3 ml 9 mol l⁻¹ HBr solution at room temperature on
189 an analogue rocker overnight. Then separated HBr solution was evaporated to dryness, with
190 the remaining Os fraction further purified by micro-distillation using the CrO₃-H₂SO₄-HBr
191 technique. The purified Os fraction was loaded onto Pt wire filament and covered with ~ 0.3
192 µl of NaOH-Ba(OH)₂ activator solution (6 mg NaOH with 20 mg Ba(OH)₂ in 1 g of ultrapure
193 H₂O) (Selby and Creaser 2001; Luguet et al., 2008). Following the extraction of Os, the acid
194 medium was evaporated to dryness with the Re fraction purified by anion exchange
195 chromatography. The eluted solution containing Re was evaporated to dryness and the Re
196 was loaded onto a Ni wire filament with ~ 0.5 µl saturated Ba(NO₃)₂ in ultrapure H₂O
197 activator solution (Creaser *et al.* 1991). The Re and Os isotope ratio measurements were
198 conducted on a Thermo Scientific TRITON mass spectrometer via ion-counting using a
199 secondary electron multiplier in peak-hopping mode for all Os and maltene Re, and static
200 Faraday collection for oil and asphaltene Re. The measured oxide ion ratios for Os and Re

201 were corrected for isobaric oxygen interferences to obtain element ratios, which were then
202 corrected for mass fractionation using a $^{192}\text{Os}/^{188}\text{Os}$ value of 3.08761 (Nier 1937) and a
203 $^{185}\text{Re}/^{187}\text{Re}$ value of 0.59738 (Gramlich *et al.* 1973), spike contributions and blank. The total
204 procedural blanks during the study are 1.90 ± 0.97 picograms for Re and 73 ± 19 femtograms
205 for Os, with an average $^{187}\text{Os}/^{188}\text{Os}$ of 0.24 ± 0.03 (internal error weighted average by *Isoplot*,
206 95% conf., $n = 7$; Table 1). An in-house Os control solution, DROsS, yields an average
207 $^{187}\text{Os}/^{188}\text{Os}$ of 0.1611 ± 0.0008 ($2 s$, $n = 126$) being identical to the reference value of
208 0.160924 ± 0.000004 ($2 s$, Luguet *et al.* 2008; Nowell *et al.*, 2008; Cumming *et al.*, 2014 and
209 references therein). The in-house Re reference solution yields an average $^{185}\text{Re}/^{187}\text{Re}$ of
210 0.5989 ± 0.0003 ($n = 116$, 95% conf.) which is used for the correction of mass fractionation
211 in comparison with the accepted $^{185}\text{Re}/^{187}\text{Re}$ value of 0.5974 (Gramlich *et al.* 1973). For each
212 sample the final expanded ($k = 2$) combined standard uncertainties presented for the Re and
213 Os data (Tables 2 - 5) were calculated by full propagation of uncertainties in weighing, blank
214 correction and spike calibrations, mass spectrometry measurements of Re and Os, and the
215 intermediate precision of the results of repeated measurements of Re and Os reference
216 solution. Additionally we also present the error correlation value (ρ) between $^{187}\text{Re}/^{188}\text{Os}$
217 and $^{187}\text{Os}/^{188}\text{Os}$ for these samples (Cumming 1969; Ludwig 1980; Schmitz and Schoene
218 2007).

219

220 **4 Results and discussion**

221

222 The Re and Os mass fractions and $^{187}\text{Re}/^{188}\text{Os}$ and $^{187}\text{Os}/^{188}\text{Os}$ values are presented in Tables
223 2 - 5 and Figure 1 - 5. For the entire Re-Os data set for each sample type (e.g., whole oil,
224 asphaltene, maltene, homogenised asphaltene powder) the standard deviation (s) and the

225 relative standard deviation (RSD), or coefficient of variation (CV) are included as an estimate
226 of data intermediate precision. Linearized probability plots are constructed with *Isoplot* (v
227 4.15). A normal distribution of the results is expected if sufficient data are obtained (Meisel
228 and Moser 2004), in which case data points should be dispersed closely to a linear trend with
229 a slope of 1 on a linearized probability plot (Ludwig 2012). In addition, histograms and
230 probability density curves presented here also indicate the range and distribution pattern of
231 the Re-Os data, although their shapes depend partially on the choice of bins and axis scale.
232

233 **4.1 RM 8505 whole oil Re and Os and comparison with previous studies**

234

235 The RM 8505 whole oil Re and Os mass fractions and isotope amount ratios are presented in
236 Table 2 and Figure 1. The results of two whole oil analyses of RM 8505 by Georgiev *et al.*
237 (2016) are also presented on the figures where appropriate for comparison.

238

239 The measurement results of eighteen RM 8505 whole oil test portions in this study range
240 from 1.69 to 2.15 ng g⁻¹ Re and 21.0 to 27.0 pg g⁻¹ total Os (i.e. all Os isotopes), with the
241 ¹⁸⁷Re/¹⁸⁸Os values ranging from 435 to 474 and ¹⁸⁷Os/¹⁸⁸Os compositions from 1.48 to 1.54.

242 The mean values are 1.95 ± 0.06 ng g⁻¹ for Re, 24.4 ± 0.8 pg g⁻¹ for Os, 454 ± 5 for
243 ¹⁸⁷Re/¹⁸⁸Os and 1.52 ± 0.01 for ¹⁸⁷Os/¹⁸⁸Os (n = 18, 95% conf.). These mean values are very

244 similar to the median values, thus indicating a symmetrical distribution of the data. The

245 linearized probability plots of the Re-Os data show that the Re-Os mass fraction and isotope
246 amount ratio data points are distributed along linear trends with slopes of ~ 1 (0.95 ~ 1.02)

247 indicating a similar to normal distribution of the data set. The histograms and the probability

248 density curves of the isotope amount ratios are clearly similar to normal distributions,

249 although this is less so for the Re and Os mass fractions. Besides the choice of the bins, the

250 less than normal distribution of the Re and Os mass fraction data is also due to the higher
251 precision of the isotope amount ratios compared to the Re and Os mass fractions, which is
252 also reflected by the lower RSD values for isotope amount ratio measurements.
253

254 The RM 8505 crude oil has also previously been analysed for Re-Os data by Sen and
255 Peucker-Ehrenbrink (2014) and Georgiev *et al.* (2016). Although slightly different methods
256 were applied, the results of these studies are consistent with the results of the present study.
257 These studies both applied HPA-S digestion instead of the Carius tube method. In addition,
258 Sen and Peucker-Ehrenbrink (2014) also sparged the OsO₄ of the digested solution directly
259 into MC-ICPMS for the measurement of ¹⁸⁷Os/¹⁸⁸Os values. The six measurements on 150 –
260 200 mg of RM 8505 by Sen and Peucker-Ehrenbrink (2014) yield Re and Os mass fractions
261 of $2.9 \pm 1.5 \text{ ng g}^{-1}$ and $28 \pm 4 \text{ pg g}^{-1}$, respectively, with ¹⁸⁷Os/¹⁸⁸Os values of 1.62 ± 0.15 (1 s,
262 n = 6; Table 2). Although spreading over a relatively large range due to the incomplete
263 digestion as indicated by the authors, the results are broadly consistent with the results of the
264 present study. The measurement results of two test portions of RM 8505 (~ 300 mg) for Re
265 and Os mass fractions of Georgiev *et al.* (2016) are slightly higher than the present study
266 (2.28 and 2.30 vs $1.95 \pm 0.25 \text{ ng g}^{-1}$ Re; ~ 31.0 and 29.3 vs $24.4 \pm 3.5 \text{ pg g}^{-1}$ Os). However,
267 the ¹⁸⁷Os/¹⁸⁸Os compositions are indistinguishable (1.455 and 1.515 vs 1.52 ± 0.04), with
268 only one of the ¹⁸⁷Re/¹⁸⁸Os values being nominally lower than this study (419 and 443 vs 454
269 ± 20). Combining the results of Georgiev *et al.* (2016) with this study, the Re-Os
270 measurement on twenty test portions of RM 8505 gives mean values of $1.98 \pm 0.07 \text{ ng g}^{-1}$ of
271 Re, $25.0 \pm 1.1 \text{ pg g}^{-1}$ of Os, 452 ± 6 of ¹⁸⁷Re/¹⁸⁸Os and 1.51 ± 0.01 of ¹⁸⁷Os/¹⁸⁸Os (n = 20, 95%
272 conf.).

273 4.2 Rhenium and Os data of the individually separated asphaltene and maltene 274 from RM 8505

275

276 The Re and Os mass fractions and $^{187}\text{Re}/^{188}\text{Os}$ and $^{187}\text{Os}/^{188}\text{Os}$ values of the individually
277 separated asphaltene and maltene samples (eighteen of each type) from the RM 8505 whole
278 oil are presented in Tables 3 and 4, and Figures 2 and 3, respectively. The asphaltene fraction
279 possesses Re and total Os mass fractions from 13.47 to 14.56 ng g^{-1} and from 137.3 to 153.2
280 pg g^{-1} , respectively. The $^{187}\text{Re}/^{188}\text{Os}$ and $^{187}\text{Os}/^{188}\text{Os}$ measurement results of the asphaltene
281 range from 543 to 570 and 1.57 to 1.65, respectively. The mean values are $14.04 \pm 0.18 \text{ ng g}^{-1}$
282 for Re, $145.4 \pm 2.4 \text{ pg g}^{-1}$ for total Os, 556 ± 4 for $^{187}\text{Re}/^{188}\text{Os}$ and 1.61 ± 0.01 for $^{187}\text{Os}/^{188}\text{Os}$
283 ($n = 18$, 95% conf.). The maltene fractions possess 0.22 to 0.27 ng g^{-1} Re and from 7.8 to 8.9
284 pg g^{-1} total Os, with $^{187}\text{Re}/^{188}\text{Os}$ values between 148 and 183 and $^{187}\text{Os}/^{188}\text{Os}$ compositions
285 between 1.09 and 1.28. The mean values are $0.25 \pm 0.01 \text{ ng g}^{-1}$ for Re, $8.4 \pm 0.2 \text{ pg g}^{-1}$ for
286 total Os, 161 ± 6 for $^{187}\text{Re}/^{188}\text{Os}$ and 1.20 ± 0.02 for $^{187}\text{Os}/^{188}\text{Os}$ ($n = 18$, 95% conf.). All of
287 the Re-Os data means for the asphaltene and maltene fractions are similar to the
288 corresponding median values.

289

290 The Re-Os data for the asphaltene and maltene fractions show linear trends on the linearized
291 probability plots, with slopes of ~ 1 (0.97 \sim 1.02). The histograms and the probability density
292 curves of the Re-Os mass fraction and isotope amount ratio data for the maltene fractions are
293 very similar to normal distributions. Those of asphaltene isotope amount ratios are similar to
294 normal distributions; however, more data are needed before this can be affirmed for
295 asphaltene Re and Os mass fractions. The lower RSD values of the isotopic compositions
296 indicate better data intermediate precision than for the Re and Os mass fractions for
297 asphaltenes. The RSD values of maltenes are generally higher than those of the asphaltene

298 and whole oil samples. Overall the Re and Os mass fraction RSD values decrease from
299 maltene to whole oil to asphaltene. This phenomenon indicates the increase in the data
300 intermediate precision, which corresponds to the increased levels of Re and Os mass fractions,
301 and the increase of sample to blank ratios.

302

303 **4.3 The roles of asphaltene and maltene in the RM 8505 whole oil Re-Os** 304 **systematics**

305

306 **4.3.1 Asphaltene and maltene separation of RM 8505**

307

308 The asphaltene and maltene fractions of RM 8505 account for an average of ~ 13% and ~ 79%
309 of the mass of crude oil (Table 6; Figure 6a). The mean loss of ~ 8% of sample during this
310 separation process can largely be attributed to the loss of volatile light fractions and any
311 water present during the drying of samples. For example, heating 0.3 g of RM 8505 crude oil
312 at 80 °C for 10 days resulted in a mass loss of 4.4%. Further, additional minor sample loss
313 can be accounted for during sample transfer, and additionally evaporation to remove the
314 CHCl₃ used to transfer the sample.

315

316 **4.3.2 Re and Os mass fractions and isotope amount ratio of asphaltene and** 317 **maltene**

318

319 The sums of the mass fractions of Re and Os for every pair of asphaltene and maltene
320 separated from the same oil, weighted by their mass percentage, are from 1.86 to 2.11 ng g⁻¹
321 Re and from 23.1 to 26.8 pg g⁻¹ Os (Figure 6b-c; Table 6). These values are indistinguishable

322 from the Re and Os contents of whole oil (Table 2), indicating good mass balance and no
323 significant Re or Os loss with the evaporated light fraction (Figure 6b-c). Disregarding any
324 possible Re and Os in the volatile components, i.e. taking the aforementioned sums as the Re
325 and Os mass fractions of the whole oil, the asphaltene fraction accounts for the majority of
326 the whole oil Re (~ 90%) and Os (~ 74%), with the remaining Re (~ 10%) and Os (~ 26%)
327 being bound in the maltene fraction (Table 6; Figure 6d-e). This observation is consistent
328 with previous studies (Selby *et al.* 2007; Rooney *et al.* 2012; Lillis and Selby 2013;
329 Cumming *et al.* 2014; Georgiev *et al.* 2016).

330

331 The $^{187}\text{Re}/^{188}\text{Os}$ and $^{187}\text{Os}/^{188}\text{Os}$ of the asphaltenes are closer to those of the RM 8505 crude
332 oils when compared with the maltenes (Figure 5). It is typical that the Re-Os isotope
333 systematics of whole oils are dominated by that of the asphaltene fractions as a direct result
334 of the asphaltene fraction housing the majority of the Re and Os of a crude oil (Figures 6 - 7;
335 Selby *et al.* 2007). For many of the oils studied by Selby *et al.* (2007), the asphaltene and
336 whole oil of the same crude oil exhibit very similar (within uncertainty) $^{187}\text{Re}/^{188}\text{Os}$ and
337 $^{187}\text{Os}/^{188}\text{Os}$. However, in contrast, such isotope amount ratios of the maltene fraction can be
338 similar, within uncertainty, to that of the whole oil and the asphaltene, but can also often
339 differ significantly from that of the crude oil and asphaltene. The available data show that the
340 maltene fractions can possess both lower $^{187}\text{Re}/^{188}\text{Os}$ and $^{187}\text{Os}/^{188}\text{Os}$ and/or lower
341 $^{187}\text{Re}/^{188}\text{Os}$ and similar to higher $^{187}\text{Os}/^{188}\text{Os}$ to that of the whole oil and asphaltene fraction
342 (Figure 7, this study; Selby *et al.* 2007; Georgiev *et al.* 2016). The explanation for the
343 differences in the Re-Os isotope systematics of the maltene to that of the asphaltene and
344 whole crude oil is currently not known.

345

346 The RM 8505 whole oil, asphaltene and maltene $^{187}\text{Re}/^{188}\text{Os}$ and $^{187}\text{Os}/^{188}\text{Os}$ define a line of
347 best-fit that determines a Re-Os date of 62.7 ± 5.7 Ma ($n = 54$, initial $^{187}\text{Os}/^{188}\text{Os} = 1.030 \pm$
348 0.051 , MSWD = 0.31). However, without detailed information with respect to the source of
349 RM 8505 and accurate estimates of its generation age from the source, it is challenging to
350 fully interpret the date given by the $^{187}\text{Re}/^{188}\text{Os}$ and $^{187}\text{Os}/^{188}\text{Os}$ of the whole oil, asphaltene
351 and maltene of RM 8505. This Re-Os date is older and only overlaps with the timing of the
352 initial oil generation of the Venezuelan source rocks, i.e. Early Eocene, when the uncertainty
353 is considered. As such, it is difficult to relate the Re-Os date to the known timing of any
354 geological process associated with the Venezuelan petroleum systems, i.e., oil generation and
355 the deposition of the source rock. In fact, we consider the outcome of the straight line of the
356 Re-Os isotope data merely to be the illustration of the fractionation of RM 8505 crude oil Re
357 and Os into the asphaltene and maltene fractions. However, any interpretation of the
358 collective use of the Re-Os systematics of crude oil, asphaltene, and maltene from a single oil
359 with respect to Re-Os geochronology of the petroleum system should be treated with caution
360 before a more thorough knowledge of the Re and Os geochemistry of a crude oil is obtained.
361

362 **4.4 Homogenised asphaltene**

363

364 The Re-Os data of two different batches of the homogenised asphaltene (2×12 , 2 samples
365 from each bottle) are presented in Table 5 and Figure 8. The Re-Os measurement results for
366 these asphaltene analyses range from 16.18 to 17.01 ng g^{-1} for Re and from 161.2 to 169.6 pg
367 g^{-1} for total Os, with the $^{187}\text{Re}/^{188}\text{Os}$ values being between 558 and 592 and the $^{187}\text{Os}/^{188}\text{Os}$
368 compositions being between 1.61 and 1.67. The mean values of the Re-Os data, which are
369 very similar to their medians, are 16.52 ± 0.10 ng g^{-1} for Re, 166.0 ± 0.9 pg g^{-1} for total Os,
370 574 ± 3 for $^{187}\text{Re}/^{188}\text{Os}$ and 1.64 ± 0.01 for $^{187}\text{Os}/^{188}\text{Os}$ ($n = 24$, 95% conf.). The linearized

371 probability plots, histograms and probability density curves illustrate the similar to normal
372 distribution of the data. The different Re and Os mass fractions and $^{187}\text{Re}/^{188}\text{Os}$
373 and $^{187}\text{Os}/^{188}\text{Os}$ values of the homogenised asphaltene sample to the individually separated
374 asphaltene samples is probably due to the lower asphaltene percentage of the whole oil (see
375 below).

376

377 **4.5 Comparing the suitability of whole oil, individually separated asphaltene and** 378 **homogenised asphaltene as Re-Os measurement reference materials**

379

380 Crude oil is a highly complex mixture of thousands of organic compounds and also water and
381 minerals in many cases (Berridge *et al.* 1968). The intrinsic heterogeneity of liquid crude oil
382 is a major problem for the intermediate precision of Re and Os mass fractions and isotope
383 amount ratios (Heilmann *et al.* 2009; Ventura *et al.* 2015; e.g. Fe). This is reflected by the
384 difference in Re-Os characteristics of whole oil samples in this study (Table 2). For example,
385 there is heterogeneity among the RM 8505 bottles analysed in this study: bottle A contains
386 less asphaltene and lower Re and Os mass fractions than the other bottles. In addition to the
387 heterogeneity of the Re and Os bearing organic compounds in RM 8505, different water
388 contents of the sampled oils could have also contributed to the variation of crude oil Re and
389 Os elemental mass fractions. For the results of all the 20 measurements on the RM 8505
390 crude oil (Georgiev *et al.* 2016 and this study), the relative standard deviations in the Re and
391 Os mass fractions are 7.8% and 9.5%, respectively. However, the relative standard deviations
392 of the $^{187}\text{Re}/^{188}\text{Os}$ and $^{187}\text{Os}/^{188}\text{Os}$ data are 2.8% and 1.6%, respectively, which are relatively
393 low. Although the variance seems to be high for the Re and Os mass fractions, in general the
394 results presented from the Re-Os measurements on the RM 8505 whole oil so far still fit for
395 the purpose of serving as a petroleum matrix-matched reference material for Re-Os

396 measurements, especially considering the good data quality of the $^{187}\text{Re}/^{188}\text{Os}$ and $^{187}\text{Os}/^{188}\text{Os}$
397 measurement results.

398

399 To avoid the influence of the heterogeneity of liquid oil, fine solid bitumen/asphaltene
400 powder, which is easier to homogenise and keep homogenised can be used instead. The
401 bitumen/asphaltene powder will still have typical petroleum sample Re and Os mass fractions,
402 and keep the character of generating carbon dioxide during digestion of liquid crude oil
403 samples. In fact, the ~ 90 g asphaltene in the form of homogenised fine solid powder yields
404 the lowest Re-Os mass fractions and isotopic data RSD values of all sample types in this
405 study. The precisions are also significantly reduced from the individually separated
406 asphaltenes – each of which is from ~ 1 g of crude oil in this study and subject to the
407 variation of asphaltene separation process (e.g. Table 6). This confirms the ability of solid
408 asphaltene powder to reduce the influence of liquid crude oil Re-Os heterogeneity. The
409 homogenised asphaltene can serve as a good reference material for both Re and Os mass
410 fractions and isotope amount ratio determination.

411

412 **5 Summary**

413

414 The Re-Os elemental mass fraction and isotope amount ratio data of NIST RM 8505 whole
415 oil and the homogenised asphaltene in this study, which were obtained via Carius Tube -
416 Isotope Dilution - NTIMS methodology, entitle them as suitable matrix-matched reference
417 material for petroleum Re-Os measurements. The Re-Os data and close to normal distribution
418 and the RSD values are low. The establishment of these matrix-matched reference materials

419 should facilitate inter- and intra-laboratory comparison and method validation with regards to
420 petroleum Re-Os measurements.

421

422 **Acknowledgements**

423

424 This research is supported by funding from a Total research award and a China Scholarship
425 Council grant to Junjie Liu, and a Total Endowment Fund to David Selby.

426

427 **References**

428 **Bandoniene, D., Zettl, D., Meisel, T., and Maneiko, M. (2013)**

429 Suitability of elemental fingerprinting for assessing the geographic origin of pumpkin
430 (*Cucurbita pepo* var. *styriaca*) seed oil: **Food Chemistry**, v. **136**, no. **3**, p. 1533-1542.

431

432 **Berridge, S., Thew, M., and Loriston-Clarke, A. (1968)**

433 The formation and stability of emulsions of water in crude petroleum and similar stocks:
434 **Journal of the Institute of Petroleum**, v. **54**, no. **539**, p. 333-357.

435

436 **Birck, J. L., Barman, M. R., and Capmas, F. (1997)**

437 Re-Os Isotopic Measurements at the Femtomole Level in Natural Samples: **Geostandards**
438 **and Geoanalytical Research**, v. **21**, no. **1**, p. 19-27.

439

440 **Cohen, A. S., Coe, A. L., Bartlett, J. M., and Hawkesworth, C. J. (1999)**

441 Precise Re–Os ages of organic-rich mudrocks and the Os isotope composition of Jurassic
442 seawater: **Earth and Planetary Science Letters**, v. **167**, no. **3-4**, p. 159-173.

443

444 **Cohen, A. S., and Waters, F. G. (1996)**

445 Separation of osmium from geological materials by solvent extraction for analysis by thermal
446 ionisation mass spectrometry: **Analytica Chimica Acta**, v. **332**, no. **2**, p. 269-275.

447

448 **Creaser, R. A., Papanastassiou, D. A., and Wasserburg, G. J. (1991)**

449 Negative thermal ion mass spectrometry of osmium, rhenium and iridium: **Geochimica et**
450 **Cosmochimica Acta**, v. **55**, no. **1**, p. 397-401.

451

452 **Cumming, G. L. (1969)**

453 A recalculation of the age of the solar system: **Canadian Journal of Earth Sciences**, v. **6**, no.
454 **4**, p. 719-735

455

456 **Cumming, V. M., Selby, D., and Lillis, P. G. (2012)**
457 Re–Os geochronology of the lacustrine Green River Formation: Insights into direct
458 depositional dating of lacustrine successions, Re–Os systematics and paleocontinental
459 weathering: **Earth and Planetary Science Letters**, v. **359-360**, p. 194-205.
460

461 **Cumming, V. M., Selby, D., Lillis, P. G., and Lewan, M. D. (2014)**
462 Re–Os geochronology and Os isotope fingerprinting of petroleum sourced from a Type I
463 lacustrine kerogen: Insights from the natural Green River petroleum system in the Uinta
464 Basin and hydrous pyrolysis experiments: **Geochimica et Cosmochimica Acta**, v. **138**, p.
465 32-56.
466

467 **Finlay, A. J., Selby, D., and Osborne, M. J. (2011)**
468 Re-Os geochronology and fingerprinting of United Kingdom Atlantic margin oil: Temporal
469 implications for regional petroleum systems: **Geology**, v. **39**, no. **5**, p. 475-478.
470

471 **Finlay, A. J., Selby, D., and Osborne, M. J. (2012)**
472 Petroleum source rock identification of United Kingdom Atlantic Margin oil fields and the
473 Western Canadian Oil Sands using Platinum, Palladium, Osmium and Rhenium: Implications
474 for global petroleum systems: **Earth and Planetary Science Letters**, v. **313-314**, p. 95-104.
475

476 **Finlay, A. J., Selby, D., Osborne, M. J., and Finucane, D. (2010)**
477 Fault-charged mantle-fluid contamination of United Kingdom North Sea oils: Insights from
478 Re-Os isotopes: **Geology**, v. **38**, no. **11**, p. 979-982.
479

480 **Ge, X., Shen, C., Selby, D., Deng, D., and Mei, L. (2016)**
481 Apatite fission-track and Re-Os geochronology of the Xuefeng uplift, China: Temporal
482 implications for dry gas associated hydrocarbon systems: **Geology**, v. **44**, no. **6**, p. 491-494.
483

484 **Georgiev, S. V., Stein, H. J., Hannah, J. L., Galimberti, R., Nali, M., Yang, G., and**
485 **Zimmerman, A. (2016)**
486 Re-Os dating of maltenes and asphaltenes within single samples of crude oil: **Geochimica Et**
487 **Cosmochimica Acta**, v. **179**, p. 53-75.
488

489 **Gramlich, J. W., Murphy, T. J., Garner, E. L., and Shields, W. R. (1973)**
490 Absolute isotopic abundance ratio and atomic weight of a reference sample of rhenium: **J.**
491 **Res. Natl. Bur. Stand. A**, v. **77**, p. 691-698.
492

493 **Heilmann, J., Boulyga, S. F., and Heumann, K. G. (2009)**
494 Development of an isotope dilution laser ablation ICP-MS method for multi-element
495 determination in crude and fuel oil samples: **Journal of Analytical Atomic Spectrometry**, v.
496 **24**, no. **4**, p. 385-390.
497

498 **James, K. (1990)**
499 The Venezuelan hydrocarbon habitat: **Geological Society, London, Special Publications**, v.
500 **50**, no. **1**, p. 9-35.
501

502 **James, K. (2000)**
503 The Venezuelan hydrocarbon habitat, part 1: tectonics, structure, palaeogeography and source
504 rocks: **Journal of Petroleum Geology**, v. **23**, no. **1**, p. 5-53.
505

506 **Li, C., Qu, W.-J., Wang, D.-H., Chen, Z.-H., Du, A.-D., and Zhang, C.-Q. (2011)**
507 Dissolving Experimental Research of Re-Os Isotope System for Bitumen Samples: **Rock and**
508 **Mineral Analysis**, v. **30**, no. **6**, p. 688-694.
509

510 **Lillis, P. G., and Selby, D. (2013)**
511 Evaluation of the rhenium–osmium geochronometer in the Phosphoria petroleum system,
512 Bighorn Basin of Wyoming and Montana, USA: **Geochimica et Cosmochimica Acta**, v. **118**,
513 p. 312-330.
514

515 **Ludwig, K. R. (1980)**
516 Calculation of uncertainties of U-Pb isotope data: **Earth and Planetary Science Letters**, v.
517 **46**, no. **2**, p. 212-220
518

519 **Ludwig, K. (2012)**
520 User’s manual for Isoplot version 3.75-4.15: a geochronological toolkit for Microsoft: **Excel**
521 **Berkley Geochronological Center Special Publication**, no. **5**, 76 p.
522

523 **Luguet, A., Nowell, G. M., and Pearson, D. G. (2008)**
524 $^{184}\text{Os}/^{188}\text{Os}$ and $^{186}\text{Os}/^{188}\text{Os}$ measurements by Negative Thermal Ionisation Mass
525 Spectrometry (N-TIMS): Effects of interfering element and mass fractionation corrections on
526 data accuracy and precision: **Chemical Geology**, v. **248**, no. **3**, p. 342-362.
527

528 **Mahdaoui, F., Michels, R., Reisberg, L., Pujol, M., and Poirier, Y. (2015)**
529 Behavior of Re and Os during contact between an aqueous solution and oil: Consequences for
530 the application of the Re–Os geochronometer to petroleum: **Geochimica et Cosmochimica**
531 **Acta**, v. **158**, p. 1-21.
532

533 **Mahdaoui, F., Reisberg, L., Michels, R., Hautevelles, Y., Poirier, Y., and Girard, J.-P.**
534 **(2013)**
535 Effect of the progressive precipitation of petroleum asphaltenes on the Re–Os radioisotope
536 system: **Chemical Geology**, v. **358**, p. 90-100.
537

538 **Marques, J. C. (2013)**
539 Overview on the Re-Os isotopic method and its application on ore deposits and organic-rich
540 rocks: **Geochimica Brasiliensis**, v. **26**, no. **1**, p. 49-66.
541

542 **Meisel, T., and Moser, J. (2004)**
543 Reference materials for geochemical PGE analysis: new analytical data for Ru, Rh, Pd, Os, Ir,
544 Pt and Re by isotope dilution ICP-MS in 11 geological reference materials: **Chemical**
545 **Geology**, v. **208**, no. **1-4**, p. 319-338.
546

547 **Meisel, T., Reisberg, L., Moser, J., Carignan, J., Melcher, F., and Brüggmann, G. (2003)**
548 Re–Os systematics of UB-N, a serpentinized peridotite reference material: **Chemical**
549 **Geology**, v. **201**, no. **1**, p. 161-179.
550

551 **Morgan, J., Golightly, D., and Dorrzapf, A. (1991)**
552 Methods for the separation of rhenium, osmium and molybdenum applicable to isotope
553 geochemistry: **Talanta**, v. **38**, no. **3**, p. 259-265.
554

555 **Nier, A. O. (1937)**

556 The isotopic constitution of osmium: **Physical Review**, v. 52, no. 8, p. 885.
557
558 **Nowell, G., Luguet, A., Pearson, D., and Horstwood, M. (2008)**
559 Precise and accurate $^{186}\text{Os}/^{188}\text{Os}$ and $^{187}\text{Os}/^{188}\text{Os}$ measurements by multi-collector plasma
560 ionisation mass spectrometry (MC-ICP-MS) part I: Solution analyses: **Chemical Geology**, v.
561 **248**, no. 3, p. 363-393.
562
563 **Qi, L., Gao, J.-F., Zhou, M.-F., and Hu, J. (2013)**
564 The Design of Re-usable Carius Tubes for the Determination of Rhenium, Osmium and
565 Platinum-Group Elements in Geological Samples: **Geostandards and Geoanalytical**
566 **Research**, v. 37, no. 3, p. 345-351.
567
568 **Reisberg, L., and Meisel, T. (2002)**
569 The Re-Os Isotopic System: A Review of Analytical Techniques: **Geostandards Newsletter**,
570 v. 26, no. 3, p. 249-267.
571
572 **Rooney, A. D., Selby, D., Lewan, M. D., Lillis, P. G., and Houzay, J.-P. (2012)**
573 Evaluating Re–Os systematics in organic-rich sedimentary rocks in response to petroleum
574 generation using hydrous pyrolysis experiments: **Geochimica et Cosmochimica Acta**, v. 77,
575 p. 275-291.
576
577 **Schmitz, M.D. and Schoene, B. (2007)**
578 Derivation of isotope ratios, errors, and error correlations for U-Pb geochronology using
579 ^{205}Pb - ^{135}U -(^{233}U)-spiked isotope dilution thermal ionization mass spectrometric data:
580 **Geochemistry, Geophysics, Geosystems**, v. 8, no. 8, 20 p.
581
582 **Selby, D., Creaser, R., Dewing, K., and Fowler, M. (2005)**
583 Evaluation of bitumen as a Re–Os geochronometer for hydrocarbon maturation and migration:
584 A test case from the Polaris MVT deposit, Canada: **Earth and Planetary Science Letters**, v.
585 **235**, no. 1-2, p. 1-15.
586
587 **Selby, D., and Creaser, R. A. (2001)**
588 Re-Os geochronology and systematics in molybdenite from the Endako porphyry
589 molybdenum deposit, British Columbia, Canada: **Economic Geology**, v. 96, no. 1, p. 197-
590 204.
591
592 **Selby, D., and Creaser, R. A. (2005)**
593 Direct radiometric dating of hydrocarbon deposits using rhenium-osmium isotopes: **Science**,
594 v. 308, no. 5726, p. 1293-1295.
595
596 **Selby, D., Creaser, R. A., and Fowler, M. G. (2007)**
597 Re–Os elemental and isotopic systematics in crude oils: **Geochimica et Cosmochimica Acta**,
598 v. 71, no. 2, p. 378-386.
599
600 **Sen, I. S., and Peucker-Ehrenbrink, B. (2014)**
601 Determination of Osmium Concentrations and $^{187}\text{Os}/^{188}\text{Os}$ of Crude Oils and Source Rocks
602 by Coupling High-Pressure, High-Temperature Digestion with Sparging OsO_4 into a
603 Multicollector Inductively Coupled Plasma Mass Spectrometer: **Analytical chemistry**, v. 86,
604 no. 6, p. 2982-2988.
605

606 **Shirey, S. B., and Walker, R. J. (1995)**
607 Carius tube digestion for low-blank rhenium-osmium analysis: **Analytical Chemistry**, v. **67**,
608 **no. 13**, p. 2136-2141.
609

610 **Speight, J. (2004)**
611 Petroleum Asphaltenes-Part 1: Asphaltenes, resins and the structure of petroleum: **Oil & gas**
612 **science and technology**, v. **59**, **no. 5**, p. 467-477.
613

614 **Steven, N., Creaser, R., Wulff, K., Kisters, A., Eglington, B., and Miller, J. (2015)**
615 Implications of high-precision Re-Os molybdenite dating of the Navachab orogenic gold
616 deposit, Namibia: **Geochemistry: Exploration, Environment, Analysis**, v. **15**, **no. 2-3**, p.
617 125-130.
618

619 **Summa, L., Goodman, E., Richardson, M., Norton, I., and Green, A. (2003)**
620 Hydrocarbon systems of Northeastern Venezuela: plate through molecular scale-analysis of
621 the genesis and evolution of the Eastern Venezuela Basin: **Marine and Petroleum Geology**,
622 **v. 20**, **no. 3**, p. 323-349.
623

624 **Ventura, G. T., Gall, L., Siebert, C., Prytulak, J., Szatmari, P., Hürlimann, M., and**
625 **Halliday, A. N. (2015)**
626 The stable isotope composition of vanadium, nickel, and molybdenum in crude oils: **Applied**
627 **Geochemistry**, v. **59**, p. 104-117.
628

629 **Völkening, J., T. Walczyk, and K.G. Heumann (1991)**
630 Osmium isotope ratio determination by negative thermal ion mass spectrometry: **International**
631 **Journal of Mass Spectrometry and Ion Processes**, v. **105**, **no. 2**, p. 147–159.
632

633 **Walczyk, T. (2004)**
634 TIMS versus multicollector-ICP-MS: coexistence or struggle for survival?: **Analytical and**
635 **bioanalytical chemistry**, v. **378**, **no. 2**, p. 229-231.
636

637 **Zimmerman, A., Stein, H. J., Morgan, J. W., Markey, R. J., and Watanabe, Y. (2014)**
638 Re–Os geochronology of the El Salvador porphyry Cu–Mo deposit, Chile: Tracking
639 analytical improvements in accuracy and precision over the past decade: **Geochimica et**
640 **Cosmochimica Acta**, v. **131**, p. 13-32.
641

642 Figures and tables

643 Table 1 Total procedural blanks of rhenium and osmium, and $^{187}\text{Os}/^{188}\text{Os}$ composition during the study.

644

Blank ID	Re (pg)	u	Os (fg)	u	$^{187}\text{Re}/^{188}\text{Os}$	u	$^{187}\text{Os}/^{188}\text{Os}$	u	rho
RO539-13	1.61	0.03	64.6	0.4	121	2	0.227	0.005	0.28
RO549-4	1.63	0.03	98.8	0.7	81	2	0.302	0.009	0.21
RO560-19	1.53	0.02	39.0	0.7	217	8	1.255	0.063	0.55
RO560-21	9.76	0.16	95.3	14.1	527	183	0.643	0.363	0.61
RO631-7	5.82	0.09	89.4	0.5	318	6	0.230	0.004	0.29
RO713-7	3.70	0.06	52.5	4.4	356	71	0.495	0.141	0.69
RO728-6	2.16	0.03	46.4	5.8	225	63	0.168	0.242	0.19

645

646 u: expanded ($k = 2$) combined standard uncertainties which include the uncertainties in weighing, blank correction and spike calibrations, mass
647 spectrometry measurements of Re and Os, and the intermediate precision of the results of repeated measurements of Re and Os reference
648 solution.

649 Os: all Os isotopes

650 rho: error correlation value between $^{187}\text{Re}/^{188}\text{Os}$ and $^{187}\text{Os}/^{188}\text{Os}$

651

652

653 Table 2 Rhenium and osmium mass fractions and isotope amount ratios of RM 8505 whole oil.

Sample	Re (ng g ⁻¹)	u	Total Os (pg g ⁻¹)	u	¹⁹² Os (pg g ⁻¹)	u	¹⁸⁷ Re/ ¹⁸⁸ Os	u	¹⁸⁷ Os/ ¹⁸⁸ Os	u	rho
A	1.86	0.04	22.5	0.9	7.8	0.7	474	43	1.54	0.18	0.72
A	1.69	0.04	21.0	0.9	7.3	0.7	459	42	1.53	0.18	0.72
A	1.88	0.04	23.4	0.9	8.2	0.7	458	41	1.53	0.18	0.72
A	1.84	0.04	22.9	0.9	8.0	0.7	456	41	1.53	0.18	0.72
A	1.94	0.04	24.3	1.0	8.5	0.7	455	41	1.52	0.18	0.72
A	1.77	0.04	22.2	0.9	7.8	0.7	454	42	1.53	0.18	0.72
mean of A:	1.83		22.7		7.9		459		1.53		
1 s	0.09		1.1		0.4		7		0.01		
B	2.15	0.04	27.0	1.1	9.4	0.8	454	40	1.51	0.18	0.71
B	2.06	0.04	26.0	1.0	9.1	0.8	450	40	1.49	0.18	0.71
B	2.09	0.04	26.8	1.1	9.4	0.8	442	39	1.48	0.17	0.71
mean of B:	2.10		26.6		9.3		449		1.49		
1 s	0.05		0.6		0.2		6		0.02		
C	1.94	0.04	25.0	1.0	8.8	0.8	441	40	1.51	0.18	0.71
C	1.88	0.04	23.6	0.9	8.3	0.7	453	41	1.52	0.18	0.72
C	1.88	0.04	23.6	0.9	8.2	0.7	454	41	1.54	0.18	0.72
mean of C:	1.90		24.1		8.4		449		1.52		
1 s	0.04		0.8		0.3		7		0.02		
D	1.94	0.04	24.4	1.0	8.5	0.7	454	41	1.53	0.18	0.72
D	2.03	0.04	26.3	1.0	9.2	0.8	439	39	1.49	0.18	0.71
D	1.97	0.04	25.7	1.0	9.0	0.8	435	39	1.49	0.18	0.71
mean of D:	1.98		25.5		8.9		443		1.50		
1 s	0.05		1.0		0.4		10		0.02		

E	2.05	0.04	25.4	1.0	8.9	0.8	460	41	1.53	0.18	0.72
E	2.01	0.04	24.8	1.0	8.7	0.8	461	41	1.53	0.18	0.72
E	2.06	0.04	24.8	1.0	8.7	0.8	472	42	1.49	0.18	0.72
mean of E:	2.04		25.0		8.7		464		1.52		
1 s	0.03		0.3		0.1		6		0.02		
median of all	1.94		24.6		8.6		454		1.52		
mean of all	1.95		24.4		8.5		454		1.52		
1 s of all	0.12		1.7		0.6		10		0.02		
RSD of all	6.2%		6.8%		6.9%		2.2%		1.3%		
CI	0.06		0.8		0.3		5		0.01		
Georgiev <i>et al.</i> (2016)											
SVG-1	2.30	0.03	31.0	0.1	np	np	419.0	6.9	1.455	0.007	0.170
SVG-2	2.28	0.03	29.3	0.1	np	np	442.9	7.8	1.515	0.008	0.149
combining the data of this study and Georgiev <i>et al.</i> (2016):											
median	1.96		24.8		8.6		454		1.52		
mean	1.98		25.0		8.5		452		1.51		
1 s	0.15		2.4		0.6		12		0.02		
RSD	7.8%		9.5%		6.9%		2.8%		1.6%		
CI	0.07		1.1		0.3		6		0.01		
Sen and Peucker-Ehrenbrink (2014)											
8505_1	5.1	np	21.7	0.4	np	np	np	np			0.03
8505_2	1.9	np	28.9	0.5	np	np	np	np	1.69		0.04
8505_2 repeat	np	np	27.9	0.7	np	np	np	np	1.74		0.07
8505_3	1.9	np	27.4	0.4	np	np	np	np	1.53		0.04
8505_4	2.7	np	35.6	0.5	np	np	np	np	1.67		0.03

8505_5	np	np	28.8	0.5	np	np	np	np	1.55	0.02
8505_6	np	np	27.0	0.4	np	np	np	np	1.36	0.02
mean	2.9		28						1.62	
1 <i>s</i>	1.5		4						0.15	

654

655 u: expanded ($k = 2$) combined standard uncertainties, see footnote of Table 1 for details

656 Total Os: all Os isotopes

657 rho: error correlation value between $^{187}\text{Re}/^{188}\text{Os}$ and $^{187}\text{Os}/^{188}\text{Os}$

658 1 *s*: 1 standard deviation

659 RSD: relative standard deviation, also known as coefficient of variation

660 CI: 95% confidence interval under Student-t distribution

661 np: data not present in publication

662

663

664

665 Table 3 Rhenium and osmium mass fractions and isotope amount ratios of the individually separated asphaltene from RM 8505.

666

Sample	Re (ng g ⁻¹)	u	Total Os (pg g ⁻¹)	u	¹⁹² Os (pg g ⁻¹)	u	¹⁸⁷ Re/ ¹⁸⁸ Os	u	¹⁸⁷ Os/ ¹⁸⁸ Os	u	rho
A 1	13.68	0.07	140.3	1.8	48.4	1.0	562	12	1.63	0.05	0.71
A 2	13.54	0.07	138.6	1.8	47.8	1.0	563	12	1.64	0.05	0.71
A 3	13.47	0.06	137.3	1.8	47.4	1.0	566	12	1.64	0.05	0.71
A 4	13.61	0.07	138.8	1.8	47.8	1.0	566	12	1.64	0.05	0.71
A 5	13.71	0.07	139.7	1.8	48.2	1.0	566	12	1.64	0.05	0.71
A 6	14.56	0.06	147.5	1.9	50.8	1.1	570	12	1.65	0.05	0.71
mean of A:	13.76		140.4		48.4		565		1.64		
1 s	0.40		3.6		1.2		3		0.01		
B 1	14.50	0.06	153.2	2.0	53.0	1.1	544	12	1.60	0.05	0.70
B 2	13.73	0.06	143.4	1.9	49.7	1.0	550	12	1.60	0.05	0.71
B 3	13.96	0.06	145.2	1.9	50.2	1.1	553	12	1.62	0.05	0.71
mean of B:	14.06		147.3		51.0		549		1.60		
1 s	0.40		5.2		1.8		5		0.01		
C 1	14.19	0.06	147.8	1.9	51.2	1.1	551	12	1.60	0.05	0.71
C 2	14.28	0.06	148.4	1.9	51.5	1.1	551	12	1.57	0.05	0.71
C 3	14.00	0.06	148.2	1.9	51.3	1.1	543	12	1.61	0.05	0.71
mean of C:	14.15		148.2		51.3		548		1.59		
1 s	0.14		0.3		0.2		5		0.02		
D 1	14.17	0.06	149.1	1.9	51.6	1.1	546	12	1.60	0.05	0.71
D 2	14.55	0.07	152.6	2.0	52.9	1.1	547	12	1.59	0.05	0.71
D 3	13.77	0.06	143.7	1.9	49.7	1.0	551	12	1.60	0.05	0.71
mean of D:	14.16		148.4		51.4		548		1.60		

1 s	0.39		4.5		1.6		2		0.01		
E 1	14.26	0.06	148.1	1.9	51.4	1.1	553	12	1.59	0.05	0.70
E 2	14.31	0.07	148.1	1.9	51.3	1.1	555	12	1.60	0.05	0.71
E 3	14.50	0.07	147.5	1.9	51.1	1.1	565	12	1.60	0.05	0.71
mean of E:	14.36		147.9		51.3		557		1.59		
1 s	0.13		0.3		0.1		6		0.01		
median of all	14.08		147.5		50.9		553		1.60		
mean of all	14.04		145.4		50.3		556		1.61		
1 s of all	0.37		4.8		1.7		9		0.02		
RSD of all	2.6%		3.3%		3.5%		1.6%		1.3%		
CI	0.18		2.4		0.9		4		0.01		

667

668 u: expanded (k = 2) combined standard uncertainties, see footnote of Table 1 for details

669 Total Os: all Os isotopes

670 rho: error correlation value between $^{187}\text{Re}/^{188}\text{Os}$ and $^{187}\text{Os}/^{188}\text{Os}$

671 1 s: 1 standard deviation

672 RSD: relative standard deviation, also known as coefficient of variation

673 CI: 95% confidence interval under Student-t distribution

674

675

676

677 Table 4 Rhenium and osmium mass fractions and isotope amount ratios of the individually separated maltene from RM 8505.

678

Sample	Re (ng g ⁻¹)	u	Total Os (pg g ⁻¹)	u	¹⁹² Os (pg g ⁻¹)	u	¹⁸⁷ Re/ ¹⁸⁸ Os	u	¹⁸⁷ Os/ ¹⁸⁸ Os	u	rho
A 1	0.25	0.04	8.1	0.4	2.9	0.3	173	34	1.25	0.19	0.52
A 2	0.26	0.04	8.7	0.4	3.1	0.3	163	32	1.21	0.18	0.50
A 3	0.25	0.04	7.8	0.4	2.8	0.3	179	36	1.22	0.19	0.53
A 4	0.27	0.04	8.7	0.4	3.1	0.3	172	32	1.22	0.18	0.52
A 5	0.27	0.04	8.1	0.4	2.9	0.3	183	35	1.28	0.19	0.54
A 6	0.27	0.04	8.2	0.4	3.0	0.3	183	35	1.24	0.18	0.54
mean of A:	0.26		8.3		3.0		176		1.24		
1 s	0.01		0.4		0.1		8		0.03		
B 1	0.23	0.04	8.2	0.4	3.0	0.4	155	36	1.22	0.19	0.48
B 2	0.23	0.04	8.1	0.4	2.9	0.4	153	33	1.18	0.18	0.48
B 3	0.23	0.04	8.4	0.4	3.1	0.4	148	31	1.13	0.17	0.47
mean of B:	0.23		8.2		3.0		152		1.18		
1 s	0.00		0.2		0.1		4		0.04		
C 1	0.24	0.04	8.7	0.4	3.1	0.4	154	31	1.19	0.17	0.48
C 2	0.23	0.04	8.6	0.4	3.1	0.4	150	31	1.20	0.18	0.48
C 3	0.24	0.04	8.7	0.4	3.2	0.4	148	29	1.16	0.17	0.48
mean of C:	0.24		8.6		3.1		150		1.18		
1 s	0.01		0.1		0.0		3		0.02		
D 1	0.22	0.04	8.2	0.4	3.0	0.3	149	32	1.09	0.16	0.47
D 2	0.25	0.04	8.7	0.5	3.1	0.4	158	33	1.22	0.18	0.49
D 3	0.24	0.04	8.5	0.4	3.1	0.4	152	31	1.18	0.17	0.48
mean of D:	0.24		8.5		3.1		153		1.16		

1 s	0.01		0.3		0.1		5		0.07		
E 1	0.24	0.04	8.0	0.4	2.9	0.4	162	33	1.22	0.18	0.50
E 2	0.24	0.04	8.9	0.4	3.2	0.4	148	30	1.20	0.17	0.48
E 3	0.27	0.04	8.8	0.4	3.2	0.3	167	31	1.18	0.17	0.51
mean of E:	0.25		8.6		3.1		159		1.20		
1 s	0.02		0.5		0.2		10		0.02		
median of all	0.24		8.5		3.1		157		1.21		
mean of all	0.25		8.4		3.0		161		1.20		
1 s of all	0.02		0.3		0.1		12		0.04		
RSD of all	6.7%		3.9%		4.0%		7.7%		3.7%		
CI	0.01		0.2		0.1		6		0.02		

679

680 u: expanded (k = 2) combined standard uncertainties, see footnote of Table 1 for details

681 Total Os: all Os isotopes

682 rho: error correlation value between $^{187}\text{Re}/^{188}\text{Os}$ and $^{187}\text{Os}/^{188}\text{Os}$

683 1 s: 1 standard deviation

684 RSD: relative standard deviation, also known as coefficient of variation

685 CI: 95% confidence interval under Student-t distribution

686

687

688

689 Table 5 Rhenium and osmium mass fractions and isotope amount ratios of the homogenised asphaltene.

690

Sample	Re (ng g ⁻¹)	u	Total Os (pg g ⁻¹)	u	¹⁹² Os (pg g ⁻¹)	u	¹⁸⁷ Re/ ¹⁸⁸ Os	u	¹⁸⁷ Os/ ¹⁸⁸ Os	u	rho
A1	16.73	0.06	166.9	1.6	57.6	0.7	578	8	1.64	0.03	0.71
A1'	16.67	0.06	167.3	1.5	57.5	0.7	576	7	1.67	0.03	0.71
A2	16.88	0.06	167.3	1.6	57.7	0.7	582	8	1.64	0.03	0.71
A2'	16.33	0.06	165.2	1.4	56.9	0.7	571	7	1.65	0.03	0.71
A3	16.33	0.06	161.2	1.5	55.5	0.7	585	8	1.65	0.03	0.71
A3'	16.18	0.06	162.6	1.4	56.1	0.7	574	7	1.64	0.03	0.71
A4	16.28	0.06	162.8	1.5	56.1	0.7	577	8	1.64	0.03	0.71
A4'	16.46	0.08	168.0	1.5	57.9	0.8	566	8	1.65	0.03	0.72
A5	16.30	0.06	165.0	1.5	56.8	0.7	570	8	1.65	0.03	0.71
A5'	16.45	0.06	166.6	1.5	57.4	0.7	570	7	1.65	0.03	0.71
A6	16.72	0.06	166.9	1.6	57.7	0.7	577	8	1.61	0.03	0.71
A6'	16.40	0.06	165.6	1.4	57.1	0.7	572	7	1.64	0.03	0.71
A7	16.32	0.06	167.6	1.6	57.9	0.7	561	7	1.62	0.03	0.71
A7'	17.00	0.06	165.8	1.4	57.2	0.7	592	7	1.64	0.03	0.71
A8	16.75	0.06	166.1	1.6	57.2	0.7	582	8	1.65	0.03	0.71
A8'	16.50	0.06	169.0	1.5	58.3	0.7	563	7	1.63	0.03	0.71
A9	16.52	0.06	167.1	1.6	57.6	0.7	571	8	1.65	0.03	0.71
A9'	17.01	0.06	169.6	1.5	58.5	0.7	578	7	1.64	0.03	0.71
A10	16.37	0.06	165.9	1.6	57.2	0.7	569	8	1.64	0.03	0.71
A10'	16.52	0.06	166.0	1.4	57.2	0.7	575	7	1.65	0.03	0.71
A11	16.40	0.06	164.9	1.5	56.9	0.7	574	8	1.64	0.03	0.71
A11'	16.67	0.06	163.7	1.4	56.4	0.7	588	7	1.65	0.03	0.71
A12	16.32	0.06	163.8	1.5	56.5	0.7	574	8	1.63	0.03	0.71
A12'	16.44	0.06	169.5	1.5	58.7	0.7	558	7	1.61	0.03	0.70
median	16.46		166.1		57.2		574		1.64		

mean	16.52	166.0	57.2	574	1.64
1 s	0.23	2.1	0.8	8	0.01
RSD	1.4%	1.3%	1.3%	1.4%	0.7%
CI	0.10	0.9	0.3	3	0.01

691

692 u: expanded (k = 2) combined standard uncertainties, see footnote of Table 1 for details

693 Total Os: all Os isotopes

694 rho: error correlation value between $^{187}\text{Re}/^{188}\text{Os}$ and $^{187}\text{Os}/^{188}\text{Os}$

695 1 s: 1 standard deviation

696 RSD: relative standard deviation, also known as coefficient of variation

697 CI: 95% confidence interval under Student-t distribution

698

699

700

701 Table 6 Asphaltene and maltene mass percentage and the proportions of their total Re and Os contents, i.e. those of the whole oil of RM 8505

702 (regardless of the lost fractions)

703

sample	fractions (%)			Total of asphaltene and maltene			asphaltene percentage (%)		maltene percentage (%)	
	asphaltene	maltene	loss	Re (ng g ⁻¹)	Os (pg g ⁻¹)	¹⁸⁷ Os (pg g ⁻¹)	Re	Os	Re	Os
A 1	12.2	79.8	8.0	1.87	23.5	4.0	89.2	72.6	10.8	27.4
A 2	12.5	77.6	9.9	1.89	24.1	4.0	89.5	72.0	10.5	28.0
A 3	12.3	79.3	8.4	1.86	23.1	3.9	89.2	73.3	10.8	26.7
A 4	12.1	79.6	8.2	1.87	23.8	4.0	88.4	70.9	11.6	29.1
A 5	12.1	80.0	7.9	1.88	23.4	4.0	88.5	72.2	11.5	27.8
A 6	11.2	82.3	6.5	1.86	23.3	3.9	87.9	70.9	12.1	29.1
the range of A whole oil values (Table 2):				1.69 - 1.94	21.0 - 24.3	3.5 - 4.1				
B 1	13.3	78.4	8.3	2.11	26.8	4.5	91.4	76.1	8.6	23.9
B 2	13.4	79.2	7.4	2.02	25.6	4.2	91.1	75.0	8.9	25.0
B 3	12.9	83.8	3.3	1.99	25.8	4.2	90.4	72.6	9.6	27.4
the range of B whole oil values (Table 2):				2.06 - 2.15	26.0 - 27.0	4.3 - 4.5				
C 1	13.5	78.8	7.7	2.10	26.7	4.4	90.9	74.4	9.1	25.6
C 2	13.1	77.7	9.3	2.05	26.0	4.3	91.2	74.5	8.8	25.5
C 3	13.3	77.7	9.0	2.04	26.4	4.4	91.0	74.4	9.0	25.6
the range of C whole oil values (Table 2):				1.88 - 1.94	23.6 - 25.0	4.0 - 4.2				
D 1	13.3	76.6	10.1	2.06	26.1	4.3	91.7	76.1	8.3	23.9
D 2	13.0	78.6	8.4	2.09	26.7	4.4	90.6	74.3	9.4	25.7
D 3	13.4	79.2	7.4	2.03	25.9	4.3	90.8	74.0	9.2	26.0
the range of D whole oil values (Table 2):				1.94 - 2.03	24.4 - 26.3	4.1 - 4.3				

E 1	12.9	81.1	6.0	2.03	25.6	4.2	90.6	74.6	9.4	25.4
E 2	13.2	79.4	7.4	2.07	26.5	4.4	90.8	73.4	9.2	26.6
E 3	13.0	77.9	9.1	2.09	26.0	4.3	90.0	73.6	10.0	26.4
	the range of E whole oil values (Table 2):			2.01 - 2.06	24.8 - 25.4	4.1 - 4.3				
	the range of all whole oil values (Table 2):			1.69 - 2.15	21.0 - 27.0	3.5 - 4.5				
median	13.0	79.2	8.1	2.03	25.8	4.2	90.6	73.8	9.4	26.2
mean	12.8	79.3	7.9	1.99	25.3	4.2	90.2	73.6	9.8	26.4
1 s	0.006	0.017	0.016	0.09	1.3	0.2	0.011	0.015	0.011	0.015
RSD	4.7%	2.2%	19.7%	4.8%	5.3%	4.5%	1.2%	2.1%	11.5%	5.8%
CI	0.3%	0.9%	0.8%	0.05	0.7	0.1	0.6%	0.8%	0.6%	0.8%

704

705 1 s: 1 standard deviation

706 RSD: relative standard deviation, also known as coefficient of variation

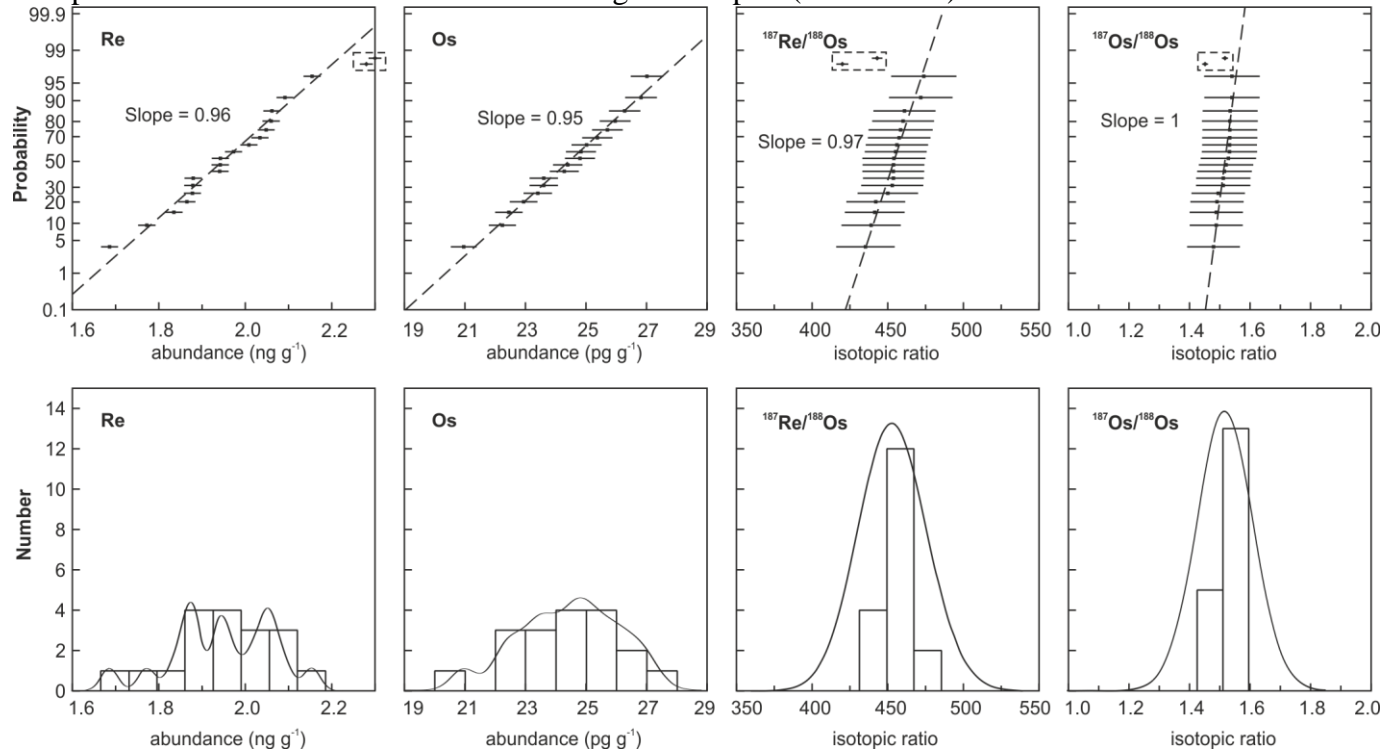
707 CI: 95% confidence interval under Student-t distribution

708

709

710

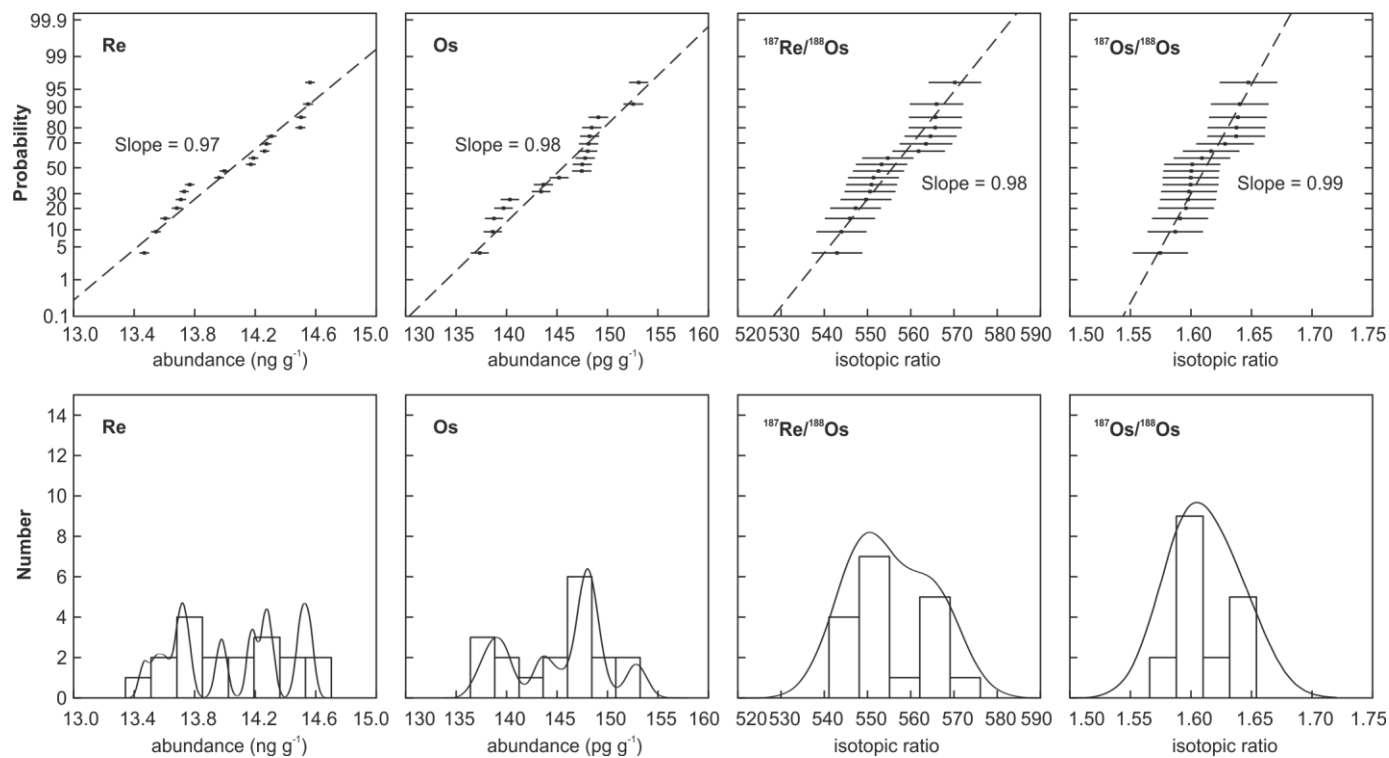
711 Figure 1 Linearized probability plots (top) and histograms and probability density curves (bottom) of RM 8505 whole oil Re-Os data. The Os
 712 data represents the total Os mass fraction. The linearized probability data points are plotted with the 1 s level combined measurement
 713 uncertainties of the measurement process. Two whole oil sample Re-Os results from Georgiev *et al.* (2016) are also plotted (in the dashed boxes)
 714 except the Os data as the values exceed the range of the plot (see Table 2).



715

716

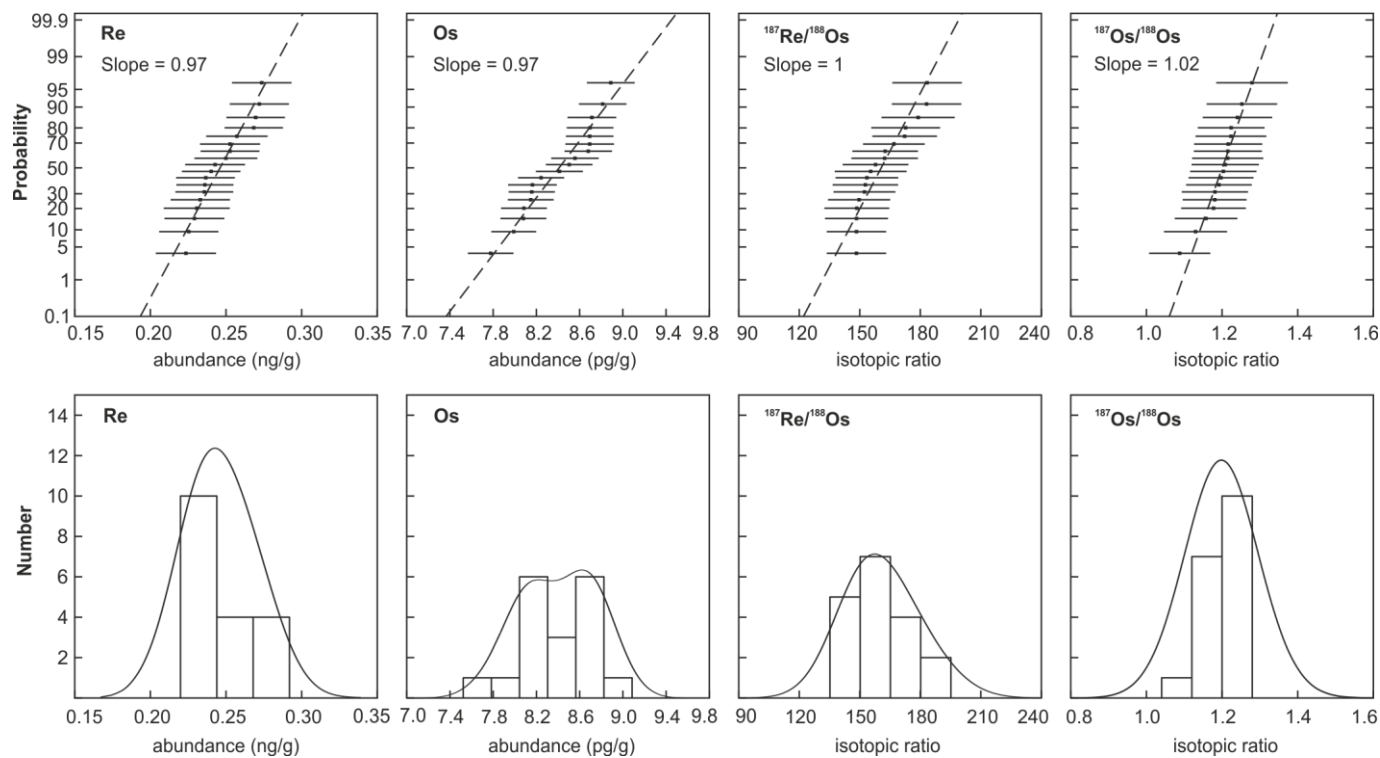
717 Figure 2 Linearized probability plots (top) and histograms and probability density curves (bottom) for individually separated asphaltene Re-Os
718 data. The Os data represents the total Os mass fraction (i.e. all Os isotopes). The linearized probability data points are plotted with the 1 σ level
719 combined measurement uncertainties of the measurement process (see Table 3).



720

721

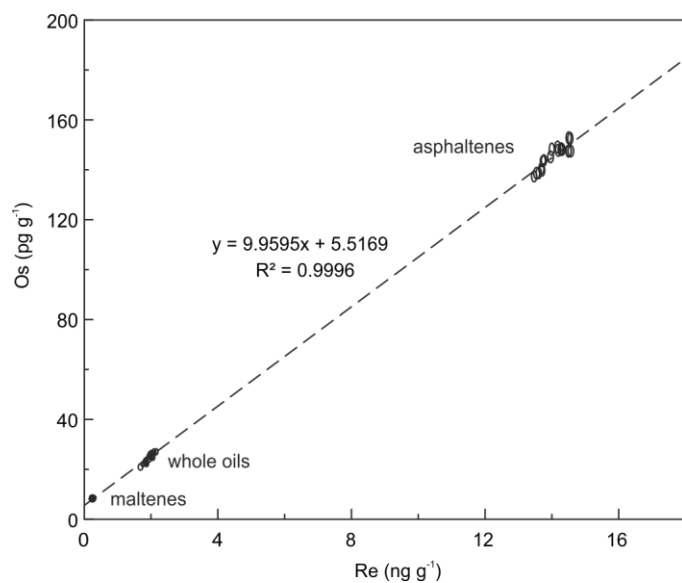
722 Figure 3 Linearized probability plots (top) and histograms and probability density curves (bottom) of separated maltene Re-Os data. Os data are
723 for total Os. The linearized probability data points are plotted with the 1 s level combined measurement uncertainties of the measurement
724 process(see Table 4).



725

726

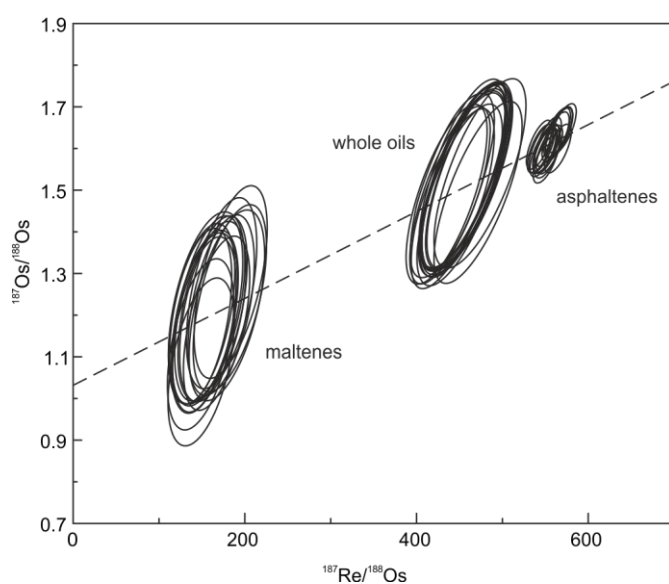
727 Figure 4 Comparison of the Re and Os mass fractions of RM 8505 whole oil, asphaltene and
728 maltene. Data-point error ellipses are the 2 s level combined measurement uncertainties of the
729 measurement process.



730

731

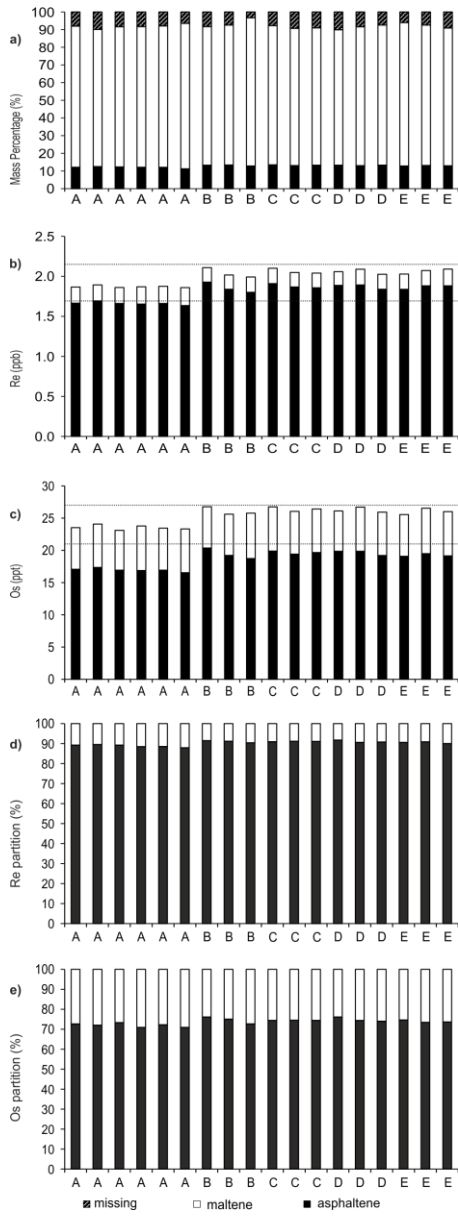
732 Figure 5 Comparison of the Re-Os isotopic compositions of the RM 8505 whole oil,
733 asphaltene and maltene. Data-point error ellipses are the 2 σ level combined measurement
734 uncertainties of the measurement process. Regression of the Re-Os data of the whole oil,
735 asphaltene and maltene fractions yields a date of 62.7 ± 5.7 Ma (initial $^{187}\text{Os}/^{188}\text{Os} = 1.030 \pm$
736 0.051 , MSWD = 0.31). We note that this date value likely does not bear any geological
737 meaning in regard to the timing of oil generation of Venezuelan petroleum systems (see text
738 for discussion).



739

740

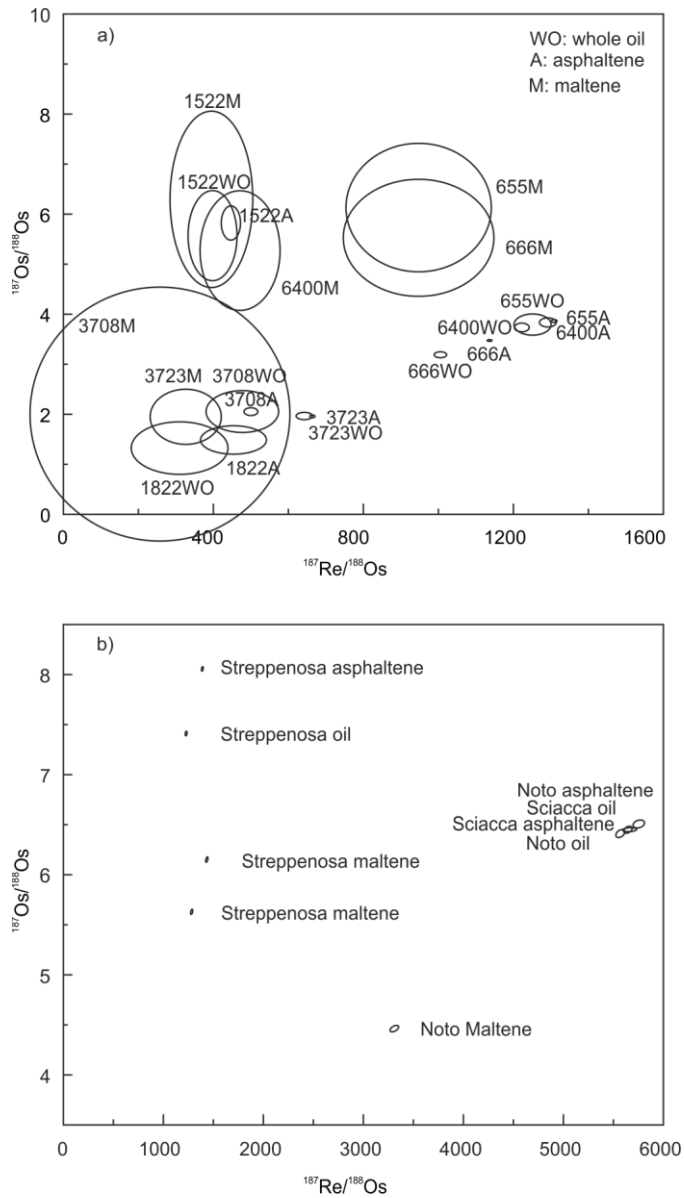
741 Figure 6 Mass balance of asphaltene-maltene separation and Re-Os budget of RM 8505 oil: a)
742 mass percentages of asphaltene and maltene; b) Re budget of RM 8505 oil separated
743 asphaltene and maltene fractions, i.e. $Total\ Re = asphaltene\ Re\ abundances \times$
744 $asphaltene\ mass\ fraction + maltene\ Re\ abundances \times maltene\ mass\ fraction$; c)
745 Os budget of RM 8505 oil separated asphaltene and maltene fractions, i.e. $Total\ Os =$
746 $asphaltene\ Os\ abundances \times asphaltene\ mass\ fraction +$
747 $maltene\ Os\ abundances \times maltene\ mass\ fraction$; d) Re percentages of asphaltene and
748 maltene within oil, e.g. $maltene\ Re\ abundances \times maltene\ mass\ fraction / Total\ Re$
749 and e) Os percentages of asphaltene and maltene within oil, e.g.
750 $(maltene\ Os\ abundances \times maltene\ mass\ fraction) / (Total\ Os)$. See text for
751 discussion.



752

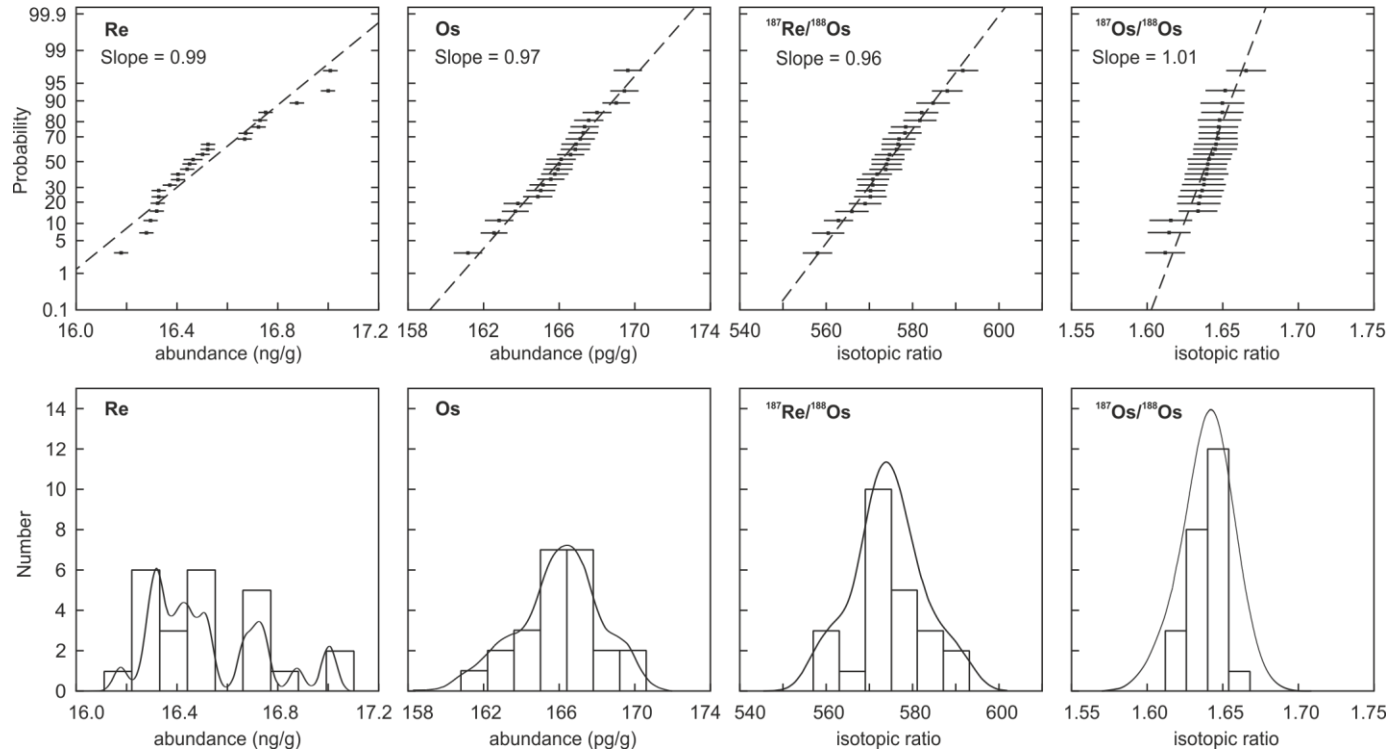
753

754 Figure 7 Comparison of the Re-Os isotopic compositions of asphaltene, crude oil and maltene
 755 of previously studied oils: a) seven oils from Selby *et al.* (2007) and b) selected data of three
 756 oils from Georgiev *et al.* (2016). Both studies utilized *n*-heptane for the separation although
 757 with slightly different protocols. See text for discussion.



758

759 Figure 8 Linearized probability plots (top) and histograms and probability density curves (bottom) of the homogenised asphaltene Re-Os data.
760 The Os data represents the total Os mass fraction. The linearized probability data points are plotted using the 1 s level combined measurement
761 uncertainties of the measurement process (see Table 5).



762